

## Organo-Soluble Porphyrin Mixed Monolayer-Protected Gold Nanorods with Intercalated Fullerenes

Chenming Xue, Yongqian Xu, Yi Pang, Dingshan Yu, Liming Dai, Min Gao, Augustine Urbas, and Quan Li

*Langmuir*, Just Accepted Manuscript • DOI: 10.1021/la300096n • Publication Date (Web): 16 Mar 2012

Downloaded from <http://pubs.acs.org> on March 20, 2012

### Just Accepted

“Just Accepted” manuscripts have been peer-reviewed and accepted for publication. They are posted online prior to technical editing, formatting for publication and author proofing. The American Chemical Society provides “Just Accepted” as a free service to the research community to expedite the dissemination of scientific material as soon as possible after acceptance. “Just Accepted” manuscripts appear in full in PDF format accompanied by an HTML abstract. “Just Accepted” manuscripts have been fully peer reviewed, but should not be considered the official version of record. They are accessible to all readers and citable by the Digital Object Identifier (DOI®). “Just Accepted” is an optional service offered to authors. Therefore, the “Just Accepted” Web site may not include all articles that will be published in the journal. After a manuscript is technically edited and formatted, it will be removed from the “Just Accepted” Web site and published as an ASAP article. Note that technical editing may introduce minor changes to the manuscript text and/or graphics which could affect content, and all legal disclaimers and ethical guidelines that apply to the journal pertain. ACS cannot be held responsible for errors or consequences arising from the use of information contained in these “Just Accepted” manuscripts.



## Report Documentation Page

*Form Approved*  
*OMB No. 0704-0188*

Public reporting burden for the collection of information is estimated to average 1 hour per response, including the time for reviewing instructions, searching existing data sources, gathering and maintaining the data needed, and completing and reviewing the collection of information. Send comments regarding this burden estimate or any other aspect of this collection of information, including suggestions for reducing this burden, to Washington Headquarters Services, Directorate for Information Operations and Reports, 1215 Jefferson Davis Highway, Suite 1204, Arlington VA 22202-4302. Respondents should be aware that notwithstanding any other provision of law, no person shall be subject to a penalty for failing to comply with a collection of information if it does not display a currently valid OMB control number.

1. REPORT DATE <b>20 MAR 2012</b>	2. REPORT TYPE	3. DATES COVERED <b>00-00-2012 to 00-00-2012</b>			
4. TITLE AND SUBTITLE <b>Organo-Soluble Porphyrin Mixed Monolayer-Protected Gold Nanorods with Intercalated Fullerenes</b>		5a. CONTRACT NUMBER			
		5b. GRANT NUMBER			
		5c. PROGRAM ELEMENT NUMBER			
6. AUTHOR(S)		5d. PROJECT NUMBER			
		5e. TASK NUMBER			
		5f. WORK UNIT NUMBER			
7. PERFORMING ORGANIZATION NAME(S) AND ADDRESS(ES) <b>Case Western Reserve University, Department of Chemical Engineering, 10900 Euclid Avenue, Cleveland, OH, 44106</b>		8. PERFORMING ORGANIZATION REPORT NUMBER			
9. SPONSORING/MONITORING AGENCY NAME(S) AND ADDRESS(ES)		10. SPONSOR/MONITOR'S ACRONYM(S)			
		11. SPONSOR/MONITOR'S REPORT NUMBER(S)			
12. DISTRIBUTION/AVAILABILITY STATEMENT <b>Approved for public release; distribution unlimited</b>					
13. SUPPLEMENTARY NOTES					
14. ABSTRACT					
15. SUBJECT TERMS					
16. SECURITY CLASSIFICATION OF:			17. LIMITATION OF ABSTRACT	18. NUMBER OF PAGES	19a. NAME OF RESPONSIBLE PERSON
a. REPORT <b>unclassified</b>	b. ABSTRACT <b>unclassified</b>	c. THIS PAGE <b>unclassified</b>			

# Organo-Soluble Porphyrin Mixed Monolayer-Protected Gold Nanorods with Intercalated Fullerenes

*Chenming Xue,<sup>†</sup> Yongqian Xu,<sup>‡</sup> Yi Pang,<sup>‡</sup> Dingshan Yu,<sup>§</sup> Liming Dai,<sup>§</sup> Min Gao,<sup>†</sup>*

*Augustine Urbas<sup>±</sup> and Quan Li<sup>\*,†</sup>*

<sup>†</sup>Liquid Crystal Institute, Kent State University, Kent, Ohio 44242, United States, <sup>‡</sup>Department of Chemistry and Maurice Morton Institute of Polymer Science, The University of Akron, Akron, Ohio 44325, United States, <sup>§</sup>Department of Chemical Engineering, Case Western Reserve University, Cleveland, Ohio 44106, United States, <sup>±</sup>Materials and Manufacturing Directorate, Air Force Research laboratory WPAFB, Ohio 45433, United States

qli1@kent.edu

**RECEIVED DATE (to be automatically inserted after your manuscript is accepted if required according to the journal that you are submitting your paper to)**

Organo-soluble porphyrin mixed monolayer-protected gold nanorods were synthesized and characterized. The resulting gold nanorods encapsulated by both porphyrin thiol and alkyl thiol on their entire surface with strong covalent Au-S linkages were very stable in organic solvents without aggregation or decomposition, and exhibited unique optical properties different from their corresponding spherical ones. Alkyl thiol acts as a stabilizer not only to fill up the potential space on gold nanorod surface between bulky porphyrin molecules, but also to provide space for further insertion of C<sub>60</sub> molecules forming a stable C<sub>60</sub>-porphyrin-gold nanorod hybrid nanostructure.

## INTRODUCTION

Building metal nanoparticles protected by functional organic molecules is a rapidly growing fascinating and challenging scientific area of contemporary interest. Gold nanorods (GNRs), providing many promising applications in optics,<sup>1</sup> sensors,<sup>2</sup> biological imaging<sup>3</sup> and anticancer agents<sup>4</sup> due to their extraordinary shape- and surface chemical environment-dependent optical properties, are among the most exciting materials today. They are quite different from the widely investigated spherical gold nanoparticles (GNPs),<sup>5</sup> including more distinguished physical properties<sup>1a,6</sup> particularly for their tunable absorption in the visible and near IR region. Besides, since anisotropic metal nanoparticles can give higher sensitivity than spherical ones in surface plasmon shift, GNRs are highly suitable for plasmon sensing with a high-value shape factor (surface curvature).<sup>7</sup> Also nanoparticle shape plays an important role in surface-enhanced Raman scattering enhancement (SERS). The enhancement factors on the order of  $10^4$ - $10^5$  were observed for absorbed molecules on the GNRs, while no such enhancement was observed on spherical nanoparticles under similar conditions.<sup>8</sup>

It is well established that modifying the chemical composition of GNR surfaces provides a versatile means to tune their properties. For example, with dye molecules on GNRs, photothermal therapy and fluorescence imaging can be accomplished simultaneously.<sup>4b</sup> Although the coupling of dye molecules and GNRs has been implemented via ionic interactions,<sup>9</sup> the dynamically unstable bilayer cetyltrimethylammonium bromide (CTAB) structure on GNRs has been a problem limiting their potential applications. In these cases, thiol molecules may have an advantage because thiol monolayer-protected GNRs exhibit superior stability, accessible surface functionalization and good compatibility with organic media, in which they can disperse well. However, to date only a few thiol monolayer-protected GNRs have been reported as the seemingly trivial work of exchanging CTAB with organic thiol molecules to form thiol-monolayer-protected GNRs is challenging.<sup>10</sup>

For chemical modification of GNRs, one class of intriguing dye molecules are porphyrins, which have been intensively studied for a range of applications over the decades due to their excellent thermal stability, charge transport ability and high light-harvesting capability.<sup>11,12</sup> It was discovered that when

1 attached to spherical GNP rather than on bulk gold surfaces, the undesirable energy transfer quenching  
2 of porphyrin's singlet excited state can be suppressed.<sup>13</sup> Furthermore, porphyrin and fullerene (C<sub>60</sub>) are  
3 an ideal donor-acceptor pair, which allows accelerated photoinduced electron transfer and slow charge  
4 recombination, leading to the generation of a long lived charge-separated state with a high quantum  
5 yield.<sup>14</sup> The porphyrin-C<sub>60</sub> assemblies can be stabilized by the attractive  $\pi$ - $\pi$  interactions.<sup>14b</sup> It is the first  
6 time to anchor them onto anisotropic gold nanoparticles and they are expected to present advantages for  
7 solar energy conversion.  
8

9  
10  
11  
12  
13  
14  
15  
16  
17 Herein we report the synthesis of GNRs that are protected by porphyrin thiol **1** and 1-decanethiol  
18 molecules via strong covalent Au-S bonds on the GNR's entire surface. The resulting mixed  
19 porphyrin/thiol monolayer-protected gold nanorods (**P-C<sub>10</sub>-GNR**) were very stable in organic solvents  
20 without aggregation or decomposition, and exhibited particular optical properties, in sharp contrast to  
21 the corresponding spherical GNPs, as well as, the porphyrin thiol **1**. The alkyl thiol C<sub>10</sub>H<sub>21</sub>SH acts as a  
22 stabilizer not only to fill up the potential space on GNR surface between bulky porphyrin molecules, but  
23 also to provide space for further insertion of C<sub>60</sub> molecules. Owing to the presence of C<sub>10</sub>H<sub>21</sub>SH  
24 molecules, the shorter alkyl chains create void space between bulky porphyrin groups for C<sub>60</sub> molecules,  
25 resulting in an electron donor-acceptor structure on the GNR surface. Together with **P-C<sub>10</sub>-GNR**, single  
26 porphyrin monolayer-protected gold nanorods (**P-GNR**), C<sub>10</sub>H<sub>21</sub>SH monolayer-protected gold nanorods  
27 (**C<sub>10</sub>-GNR**), and porphyrin monolayer-protected spherical gold nanoparticles (**P-GNP**) were also  
28 synthesized for comparison study (see supporting information). Compared with the straightforward  
29 synthesis of spherical **P-GNPs** in one step,<sup>15</sup> the preparation of thiol monolayer-protected GNRs is more  
30 complicated.  
31  
32  
33  
34  
35  
36  
37  
38  
39  
40  
41  
42  
43  
44  
45  
46  
47  
48

## 49 EXPERIMENTAL SECTION

50  
51  
52 **Materials and Measurements.** All chemicals and solvents were purchased from commercial supplies  
53 and used without further purification. HAuCl<sub>4</sub> is a 30 wt% in diluted HCl solution. <sup>1</sup>H NMR spectra  
54 were recorded on a Bruker 400 MHz NMR spectrometer, with deuterated chloroform (CDCl<sub>3</sub>) as solvent  
55 at 25 °C. The chemical shifts were reported using 7.26 ppm of CHCl<sub>3</sub> residue as the internal standard.  
56  
57  
58  
59  
60

<sup>13</sup>C NMR spectra were recorded on a Varian 200 MHz NMR spectrometer, with deuterated chloroform (CDCl<sub>3</sub>) as solvent. The chemical shifts were reported using 77.16 ppm of CHCl<sub>3</sub> residue as the internal standard. The NMR graphs and data were collected by using Spinworks 3 software. Fourier transfer infrared spectra (FTIR) were recorded on a Nicolet Magna-IR<sup>TM</sup> spectrometer 550 spectrometer at the resolution of 4 cm<sup>-1</sup>. High resolution mass spectrometry (HRMS) was performed by Mass Spectrometry & Proteomics Facility of Ohio State University. Elementary analysis was performed in Robertson Microlit Laboratories. UV-visible spectra were collected on a PerkinElmer Lambda 25 UV-Vis spectrometer at the resolution of 1 nm. Fluorescence spectra were recorded on a FluoroMax-4 spectrofluorometer of Horiba scientific. The Raman spectra are obtained with a RENISHAW inVia Raman microscope instrument using a diode laser with excitation wavelength of 785 nm. Samples for Raman spectra were casted on glass slides and left to dry before measurements. Each spectrum is obtained in 10 s collection time with five accumulations. For transmission electron microscopy (TEM) observation, solution samples were first dispersed on TEM Cu grids pre-coated with thin carbon film (Cu-400 CN) purchased from Pacific Grid Tech. After completely dried, they were studied using a FEI Tecnai TF20 FEG TEM equipped with a EDAX energy-dispersive X-ray spectrometer (EDX) for elemental analysis.

**Preparation of Porphyrin Thiol 1.** The route of preparing porphyrin thiol **1** was shown in Figure 1. The porphyrin thiol **1** was synthesized starting from unsymmetrical porphyrin derivative **2**, which was reacted with 11-bromo-1-undecanol to give bromo compound **3**. Then the active bromide **3** was reacted with potassium thiol acetate to give the intermediate compound **4**. Finally the intermediate **4** was deprotected in the presence of tetrabutylammonium cyanide (TBACN) to afford the product porphyrin thiol **1**. The structure of intermediate **2-4** was identified by <sup>1</sup>H NMR, <sup>13</sup>C NMR, Ft-IR, elemental analysis and HRMS. For **1**, because it was not able to be purified through column, the reaction product of **1** was characterized by <sup>1</sup>H NMR and HRMS, from which the yield and rightness of the compound **1** can be verified (Figure S1). The details were listed in supporting information.

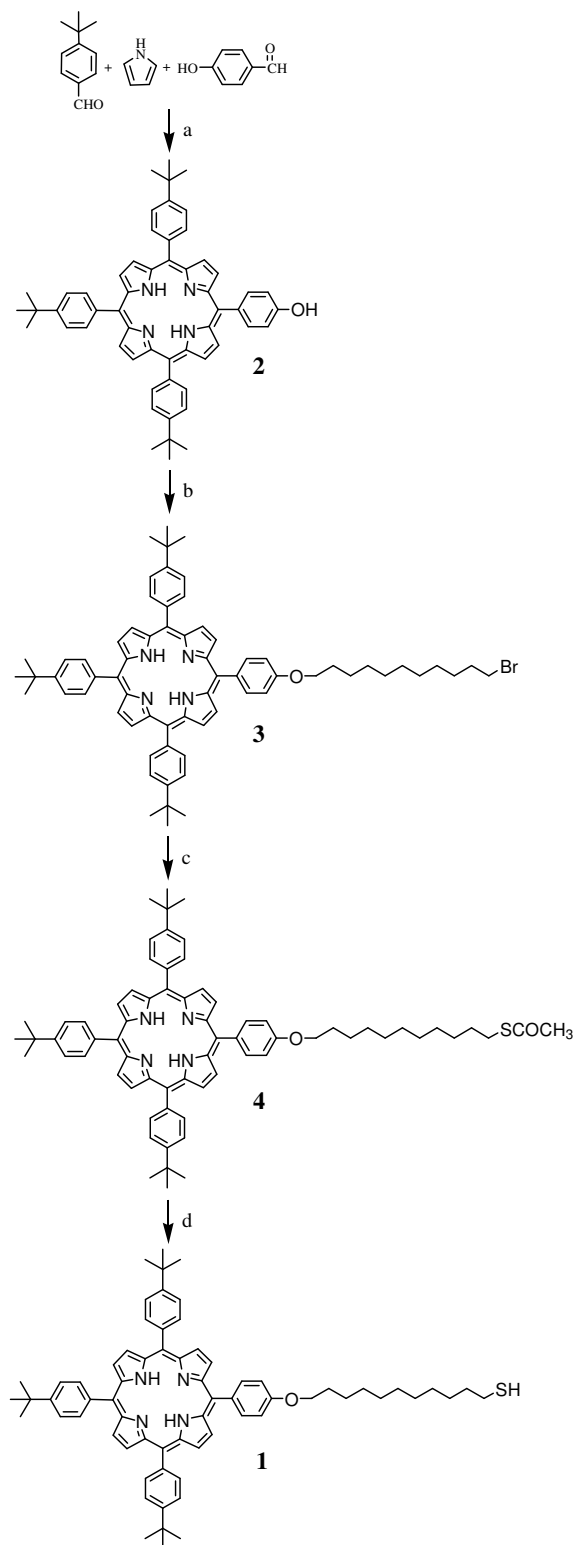


**Figure 1.** Synthesis of porphyrin thiol **1**. Conditions: (a) propionic acid, reflux; (b) 11-bromo-1-undecanol, DIAD, PPh<sub>3</sub>, stir at RT; (c) CH<sub>3</sub>COSK, acetone/CHCl<sub>3</sub> (1:1), RT, 24h; (d) tetrabutylammonium cyanide, CHCl<sub>3</sub>/MeOH (2:1), 50°C, 24h.

1  
2  
3  
4  
5  
6  
7  
8  
9  
10  
11  
12  
13  
14  
15  
16  
17  
18  
19  
20  
21  
22  
23  
24  
25  
26  
27  
28  
29  
30  
31  
32  
33  
34  
35  
36  
37  
38  
39  
40  
41  
42  
43  
44  
45  
46  
47  
48  
49  
50  
51  
52  
53

**Preparation of CTAB-Coated Gold Nanorods (CTAB-GNRs).** The CTAB-coated GNRs were freshly prepared by the seed-mediated growth method.<sup>1a</sup> For seed preparation, specifically, 0.5 mL of an aqueous 0.01 M solution of H<sub>2</sub>AuCl<sub>4</sub> was added to CTAB solution (15 mL, 0.1 M) in a vial. A bright brown-yellow color was appeared. Then, 1.20 mL of 0.01 M ice-cold aqueous NaBH<sub>4</sub> solution was added all at once, followed by rapid inversion mixing for 2 minutes. The solution developed a pale brown-yellow color. Then, the vial was kept in a water bath maintained at 25 °C for future use. For nanorods growth, 9.5 mL of 0.1 M CTAB solution in water was added to a tube, 0.40 mL of 0.01 M H<sub>2</sub>AuCl<sub>4</sub> and 0.06 mL of 0.01 M AgNO<sub>3</sub> aqueous solutions were added in this order and mixed by inversion. Then, 0.06 mL of 0.1 M of ascorbic acid solution was added and the resulting mixture at this stage becomes colorless. The seed solution (0.02 mL) was added to the above mixture tube, and the tube was slowly mixed for 10 seconds and left to sit still in the water bath at 25-30 °C for 3 h. The final solution turned purple within minutes after the tube was left undisturbed.

28  
29  
30  
31  
32  
33  
34  
35  
36  
37  
38  
39  
40  
41  
42  
43  
44  
45  
46  
47  
48  
49  
50  
51  
52  
53

**Porphyrin thiol monolayer protected gold nanorods (P-GNRs).** The solution of CTAB-GNRs was centrifuged at 7500 rpm per 20 minutes several times to remove the excessive CTAB and other solution components and redispersed in 1.5 mL of water. Then, this aqueous solution of GNRs was added dropwise to a solution of the thiol **1** (50 mg) in 40 mL THF with stirring under the protection of nitrogen. The color of the reaction mixture is purple. The reaction mixture was continued to stir at room temperature for 3 days and centrifuged. To improve the GNRs with thiol molecules over the surface, the precipitates were dispersed in CHCl<sub>3</sub> and sonicated, 10 mg thiol **1** were added into the solutions. The solution was stirred for another 24 h and centrifuged. This procedure was repeated another three times. The as-prepared GNRs were centrifuged and washed with CHCl<sub>3</sub> several times until there was no UV or <sup>1</sup>H NMR signal in the top layer solution, which means there were no free thiols in the system. The resulting GNRs were named as **P-GNRs**.

54  
55  
56  
57  
58  
59  
60

**Decanethiol monolayer protected gold nanorods (C<sub>10</sub>-GNRs).** The synthesis method was following the above, the thiol molecules C<sub>10</sub>H<sub>21</sub>SH (30 mg) was used for the first exchange and 10 mg was used for each of the next steps for complete surface protection.



1 **Porphyrin thiol and decanethiol monolayer protected gold nanorods (P-C<sub>10</sub>-GNRs).** The  
2 synthesis method was following the above, the porphyrin thiol **1** (56 mg, 0.057 mmol) was mixed with  
3 CTAB-GNR first and then C<sub>10</sub>H<sub>21</sub>SH (10 mg, 0.057 mmol) was added slowly. 5 mg **1** and 10 mg  
4 C<sub>10</sub>H<sub>21</sub>SH were used for each of the next steps for complete surface protection.  
5  
6  
7  
8

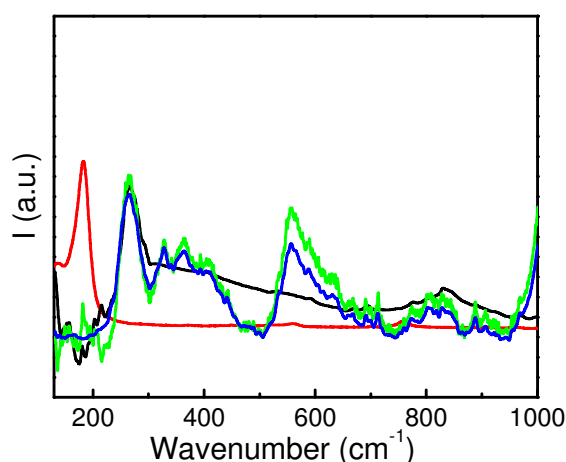
9 **Synthesis of Porphyrin-Thiol Monolayer Protected Spherical Gold Nanoparticles (P-GNPs).** The  
10 route is based on the reference<sup>15a</sup> with some modifications. An aqueous solution of hydrogen  
11 tetrachloroaurate (3 mL, 30 mmol/L) was mixed with a solution of tetraoctylammonium bromide in  
12 toluene (8 mL, 50 mmol/L). The two-phase mixture was vigorously stirred until all the tetrachloroaurate  
13 was transferred into the organic layer. The water layer was removed and 50 mg **1** was then added to the  
14 organic phase. A freshly prepared aqueous solution of sodium borohydride (2.5 mL, 0.4 mol/L) was  
15 slowly added with vigorous stirring. After further stirring for 3 h the organic phase was separated,  
16 evaporated to 1 ml in a rotary evaporator and mixed with 40 ml ethanol. The mixture was kept for 4 h at  
17 -18°C. The crude product was filtered off and washed with ethanol. The solid was dissolved in CHCl<sub>3</sub>  
18 and centrifuged at 14000 rpm for 12 min. After centrifuge, the top layer was removed and the solid was  
19 sonicated after adding CHCl<sub>3</sub>. This wash step was carried several times until the top layer does not have  
20 UV or vis absorption signal for free porphyrin molecules. Afterwards, the **P-GNP** in CHCl<sub>3</sub> was  
21 obtained.  
22  
23  
24  
25  
26  
27  
28  
29  
30  
31  
32  
33  
34  
35  
36  
37  
38  
39

40 **Preparation of C<sub>60</sub>-P-C<sub>10</sub>-GNR.** For inserting fullerenes (C<sub>60</sub>) into the **P-C<sub>10</sub>-GNR** or **P-GNR**, about  
41 0.4 mg corresponding NRs was dissolved in 2 mL of 1:1 (v/v) toluene/CH<sub>3</sub>CN. Saturated C<sub>60</sub> toluene  
42 solution (3 mg/mL) was added by drops. The mixture was stirred at room temperature. The prepared  
43 **C<sub>60</sub>-P-C<sub>10</sub>-GNR** and **C<sub>60</sub>-P-GNR** solutions were centrifuged. Then the top layer was removed, 2 mL of  
44 CHCl<sub>3</sub> was added and the mixture was sonicated. After washed with CHCl<sub>3</sub> several times until there was  
45 no UV absorption in the top layer, which means there was no free C<sub>60</sub> in the solvent. CHCl<sub>3</sub> (2 mL) was  
46 added and the solid was sonicated and dispersed well.  
47  
48  
49  
50  
51  
52  
53  
54  
55

56 **I<sub>2</sub> Induced Decomposition of P-C<sub>10</sub>-GNR.** In a typical procedure, ca. 2 mg **P-C<sub>10</sub>-GNR** were  
57 dissolved in CDCl<sub>3</sub> and its <sup>1</sup>H NMR spectrum was collected. Then, 1 mg iodine was added to this  
58  
59  
60

1 solution and followed by stirring at room temperature for 3 h. The decomposition process could be  
2 monitored by a change in solution color from purple to dark red-purple. After removal of bulky gold by  
3 centrifuging, the clear top layer solution was collected and dried. After dissolved in  $\text{CDCl}_3$ ,  $^1\text{H}$  NMR  
4 spectrum was collected and it was compared with that from before decomposition. For fluorescence  
5 experiment, since the excess  $\text{I}_2$  made the solution pink-red color, aqueous  $(\text{NH}_4)_2\text{SO}_3$  solution (0.5 M)  
6 was added to the above organic solution and it was shaken vigorously. Afterwards, the aqueous layer  
7 was removed. P-GNP and P-GNR were treated the same way for releasing porphyrin thiols.  
8  
9  
10  
11  
12  
13  
14  
15

## 16 RESULTS AND DISCUSSION



34 **Figure 2.** Raman spectra of the **CTAB-GNR** (red), **P-C<sub>10</sub>-GNR** (blue), **P-GNR** (green), and **C<sub>10</sub>-GNR**  
35 (black).  
36  
37  
38

39 Raman spectra (Figure 2) exhibited a characteristic Au-Br band at  $180\text{ cm}^{-1}$  for CTAB-coated gold  
40 nanorods (**CTAB-GNR**) and a characteristic Au-S band at  $260\text{ cm}^{-1}$  accompanied with the  
41 disappearance of Au-Br band for **P-C<sub>10</sub>-GNR**, **P-GNR** and **C<sub>10</sub>-GNR**,<sup>8,16</sup> which indicated the successful  
42 removal of bromide and covalent bonding of thiol molecule to gold surface. In order to further confirm  
43 that the thiol molecules indeed replaced CTAB molecules on GNR surface, energy-dispersive X-ray  
44 spectroscopy (EDX) was performed (Figure S2). It can be seen that the S peak appeared for **P-C<sub>10</sub>-GNR**  
45 with the disappearance of Br peak. Besides,  $^1\text{H}$  NMR (Figure 3) measurements show the peaks became  
46 broadened and weaker than the free porphyrin **1** molecules, similar to the results of other GNRs.<sup>10c</sup> The  
47 reasons for this broadening effect have been raised: (a) the tight packing of protons close to the Au core  
48 causes rapid spin-spin relaxation from dipolar interactions; (b) there are different chemical shifts for  
49 surface heterogeneities (different nanocrystalline faces: vertexes, edges, terraces), and the chemical  
50 shifts vary with core size and defect; and (c) slow rotational diffusion of the clusters (analogous to  
51  
52  
53  
54  
55  
56  
57  
58  
59  
60

effects seen for large proteins) depending on nanoparticle size.<sup>10e</sup> Although the signals of porphyrin thiols could not be observed on GNRs, they reappeared after been detached from GNRs. After degradation by adding I<sub>2</sub>, the composition of thiol molecules on **P-C<sub>10</sub>-GNR** can be calculated (Figure 3). The following is the way to calculate the ratio of porphyrin **1** to C<sub>10</sub>H<sub>21</sub>SH. In the green curve, the ratio of integration areas of aromatic part to alkyl part equals to 1:3. Since for porphyrin thiol **1** the porphyrin core part has 24 H (aromatic) and alkyl part has 50 H, we can calculate the integration of protons from C<sub>10</sub>H<sub>21</sub>SH equal to:  $3 - 1/24 \times 50 = 0.92$  from the green curve (as the integration of porphyrin aromatic H = 1). Therefore, the ratio of **1** to C<sub>10</sub>H<sub>21</sub>SH is (1/24):(0.92/22), approximately 1 : 1. Thus, it is 1:1 ratio of thiol **1** to C<sub>10</sub>H<sub>21</sub>SH on **P-C<sub>10</sub>-GNR**.

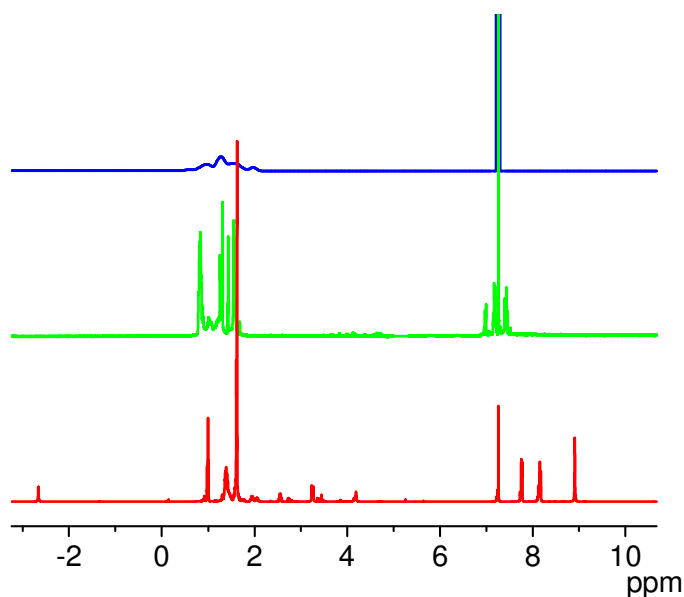
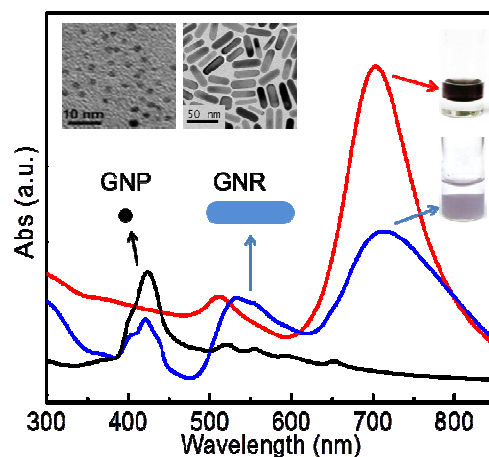


**Figure 3.** <sup>1</sup>H NMR spectra of: **P-C<sub>10</sub>-GNR** (blue), mixture residue after I<sub>2</sub> induced decomposition (green), **1** after reducing reaction (red).

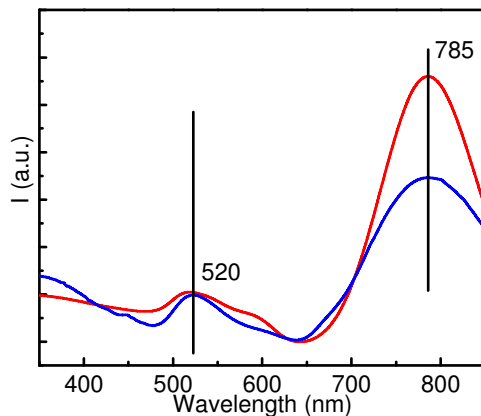


1 **Figure 4.** UV-Vis spectra of **CTAB-GNR** in H<sub>2</sub>O (red), and **P-C<sub>10</sub>-GNR** (blue) and spherical **P-GNP**  
2 (black) in CHCl<sub>3</sub>. The insets show photographs of the solutions of corresponding **CTAB-GNR** (right-  
3 top) and **P-C<sub>10</sub>-GNR** (right-bottom) in the two phases (top layer: water; bottom layer: CHCl<sub>3</sub>), and TEM  
4 images of **P-GNP** (left) and **P-C<sub>10</sub>-GNR** (right).  
5  
6  
7  
8  
9

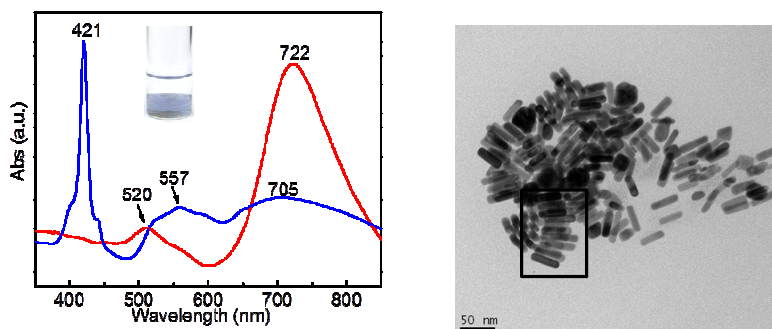
10 UV-vis absorption spectra of **CTAB-GNR**, **P-C<sub>10</sub>-GNR** and spherical **P-GNP** are shown in Figure 4.  
11 Stable organo-soluble **P-C<sub>10</sub>-GNR** and spherical **P-GNP** were observed by transmission electron  
12 microscopy (TEM), showing they were well dispersed with no aggregation (Insets in Figure 4). **P-C<sub>10</sub>-**  
13 **GNR** displayed an average size of 44 nm × 13 nm and an approximate aspect ratio of 3.4 based on a  
14 sample of 500 nanorods. Spherical **P-GNP** had an average diameter of 2.3 nm. The existence of typical  
15 porphyrin peak at 421 nm indicated the bonding of porphyrin thiol **1** on GNR. After a successful  
16 exchange with thiols, the nanoparticles were moved from aqueous media to organic solvent. In contrast  
17 to UV-vis absorption spectrum of the spherical **P-GNP**, two characteristic plasmon peaks were observed  
18 for both **CTAB-GNR** and **P-C<sub>10</sub>-GNR**. The strong longitudinal peak in the near-infrared region (710  
19 and 714 nm respectively) is corresponding to the electron oscillation along the long axis, and a weak  
20 transverse peak in the visible region (513 and 533 nm respectively) is due to electron oscillation along  
21 the short axis. The red-shift of the longitudinal and transverse peaks for **P-C<sub>10</sub>-GNR** results from the  
22 change of dielectric constant around GNR due to attachment of the porphyrin **1**. Without porphyrin **1**,  
23 **C<sub>10</sub>-GNR** did not show such red shift for either of these two peaks (Figure 5). Notably, the transverse  
24 peak shows a large red-shift (about 20 nm), which could be ascribed to the side-by-side arrangement of  
25 nanorods in solution.<sup>17</sup> However, since there was neither accompanying blue-shift of the longitudinal  
26 band, nor any prominent side-by-side assembly of GNRs observed by TEM (Inset of Figure 4 and Figure  
27 S3), the peak shift can only be attributed to the influence of porphyrin **1**. Additionally, UV-vis absorption  
28 spectra and TEM images of **P-GNR** (with only porphyrin **1** on GNR surface) were shown in Figure 6.  
29 The appearance of characteristic porphyrin peak (421 nm) indicated the binding of **1** onto these GNRs.  
30 However, its CHCl<sub>3</sub> solution displayed bluish color and UV-vis absorption spectra showed that the two  
31  
32  
33  
34  
35  
36  
37  
38  
39  
40  
41  
42  
43  
44  
45  
46  
47  
48  
49  
50  
51  
52  
53  
54  
55  
56  
57  
58  
59  
60

1  
2  
3  
4  
5  
6  
7  
8  
9  
10  
11  
12  
13  
14  
15  
16  
17  
18  
19  
20  
21  
22  
23  
24  
25  
26  
27  
28  
29  
30  
31  
32  
33  
34  
35  
36  
37  
38  
39  
40  
41  
42  
43  
44  
45  
46  
47  
48  
49  
50  
51  
52  
53  
54  
55  
56  
57  
58  
59  
60

SPR peaks broadened. Also there were significant red-shift for transverse SPR (from 520 to 557 nm) and blue shift for longitudinal SPR (from 722 to 705 nm). This implies the side-by-side assembling of GNRs, which was observed by TEM. The attractive  $\pi$ - $\pi$  interaction of porphyrin chromophores could be the interpretation for the assembly of **P-GNR**.



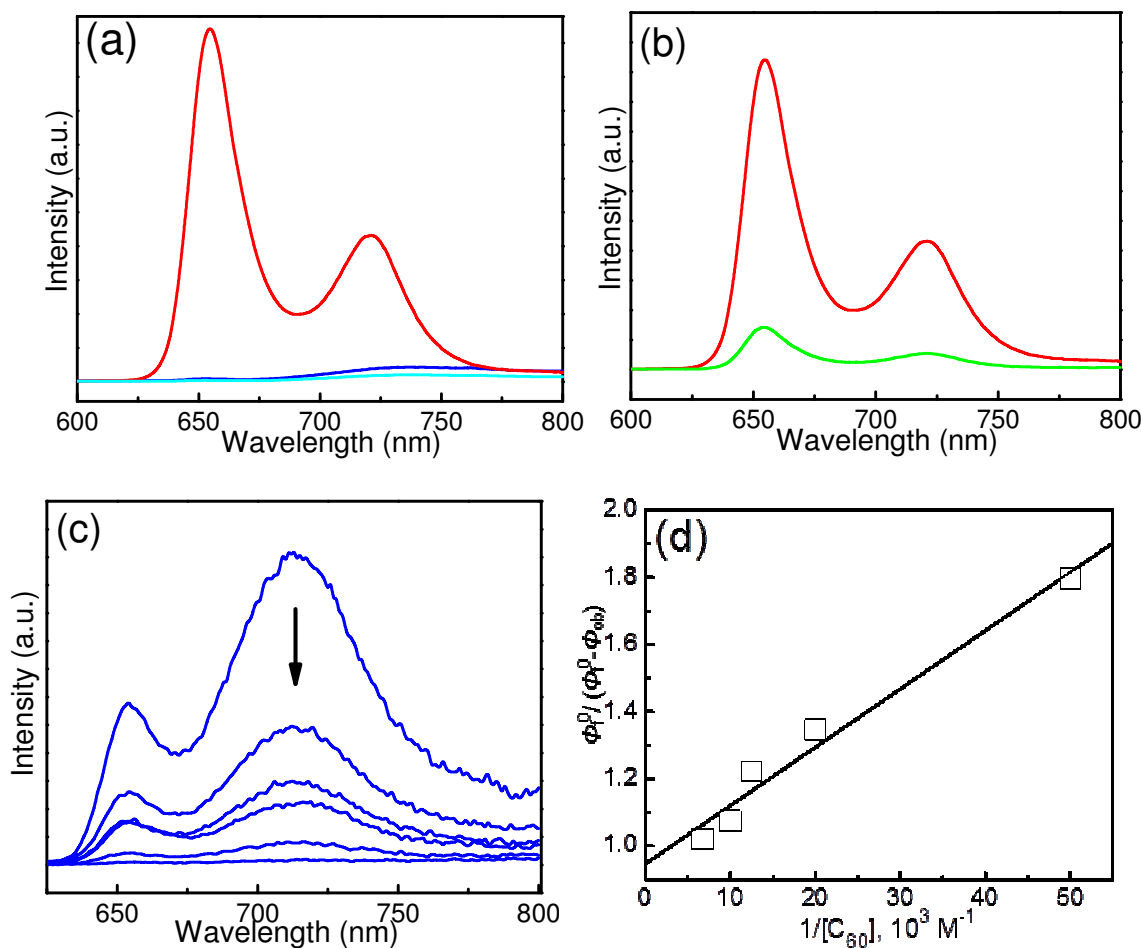
**Figure 5.** The UV-Vis spectra of **CTAB-GNR** in  $\text{H}_2\text{O}$  (red) and **C<sub>10</sub>-GNR** in  $\text{CHCl}_3$  (blue).



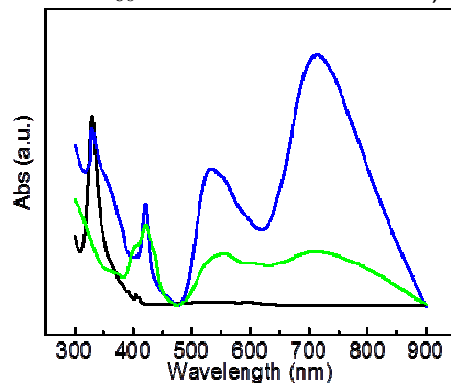
**Figure 6.** Left: UV-vis of **CTAB-GNR** (red) and **P-GNR** (blue) (Inset: the picture of **P-GNR** in  $\text{CHCl}_3$  showing bluish color, top layer is water). Right: TEM image of **P-GNR**, indicating the existence of side-by-side assembly.

Fluorescence spectra (Figure 7(a), (b) ) also revealed the distinctively different patterns for all these prepared nanoparticles. After detaching from gold nanoparticles, free porphyrin thiols in  $\text{CHCl}_3$  showed characteristic emission peaks at 656 and 721 nm. When being linked onto gold nanoparticles including GNPs and GNRs, the intensity significantly quenched, almost 99%. However, for P-GNP the peak shape was almost same as free porphyrins. For P-GNR and P-C10-GNR, the peak intensity and shape were similar. Different from free porphyrins and P-GNP, the peak at 712 nm was relatively much stronger

than the 656 nm peak. This indicated that there exist the interaction between the porphyrin and gold nanoparticles, and the photoelectronic properties of porphyrin chromophores are significantly altered when closely bound to GNRs.



**Figure 7.** (a). Fluorescence spectra of free porphyrins detached from P-C<sub>10</sub>-GNR (red) (diluted for ten times), **P-C<sub>10</sub>-GNR** (blue) and P-GNR (cyan) in CHCl<sub>3</sub> with excitation wavelength at 420 nm. For, P-GNR the intensity of free porphyrin thiols was normalized to be the same as from P-C10-GNR. (b) Fluorescence spectra of free porphyrins detached from P-GNP (red) (diluted for ten times), **P-GNP** (green) in CHCl<sub>3</sub> with excitation wavelength at 420 nm. (c): The quench of **P-C<sub>10</sub>-GNR** in 1:1 (v/v) toluene/CH<sub>3</sub>CN (0.2 mg in 2 mL mixture) upon the addition of C<sub>60</sub> (C<sub>60</sub> concentrations from top to bottom: 0 mM, 0.02 mM, 0.05 mM, 0.08 mM, 0.1 mM and 0.15 mM). (d) Dependence of  $\Phi_f^0 / (\Phi_f^0 - \Phi_f^{(ob)})$  on the reciprocal concentration of C<sub>60</sub> in acetonitrile/toluene ) 1/1.



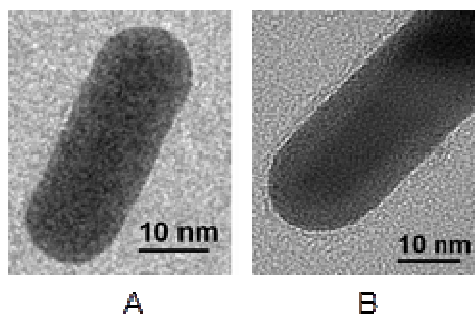


**Figure 8.** (Top): UV-vis spectra of **P-C<sub>10</sub>-GNR** (blue) and **P-GNR** (green) after washing away free C<sub>60</sub> in solution. Solution of C<sub>60</sub> (black) has also been presented for referring. (Bottom) TEM images of **P-C<sub>10</sub>-GNR** (A) and **C<sub>60</sub>-P-C<sub>10</sub>-GNR** conjugate. Note: The diffusion layer on the edge of **P-C<sub>10</sub>-GNR** (B) indicates the existence of C<sub>60</sub> molecules.

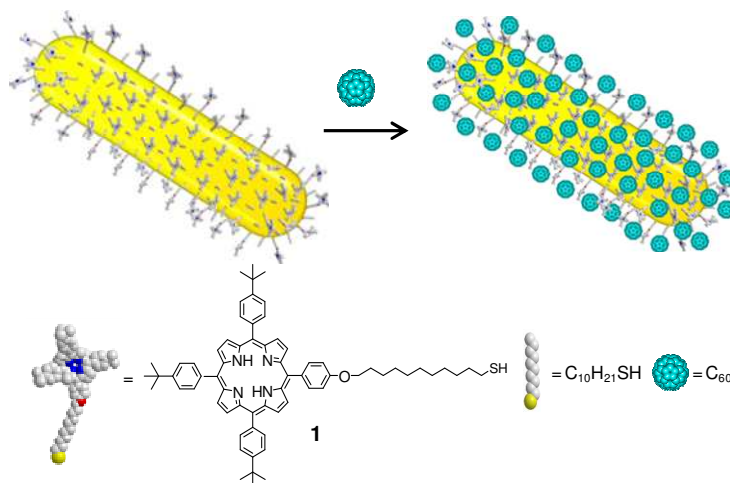
The formation of C<sub>60</sub>-GNR conjugations was verified by further fluorescence quenching in toluene/CH<sub>3</sub>CN mixture for **P-C<sub>10</sub>-GNR** in Figure 7(c), even though the fluorescence of porphyrin chromophores has been significantly quenched by GNRs. (The association constant for the formation of **P-C<sub>10</sub>-GNR** and C<sub>60</sub> complex has been calculated based on the fluorescence quenching in Figure 7 (c) and (d). After simplified treatment,<sup>18</sup> the formular is:

$$\frac{1}{\Phi_f^0 - \Phi_{f(ob)}^0} = \frac{1}{\Phi_f^0 - \Phi_f'} + \frac{1}{K(\Phi_f^0 - \Phi_f')[C_{60}]}$$

$\Phi_f^0$  is the fluorescence quantum yield of uncomplexed P-C<sub>10</sub>-GNR,  $\Phi_f'$  is the complexed one,  $\Phi_{f(ob)}^0$  is the observed yield and  $K$  is the association constant.  $\Phi_f'$  is considered as 0 when complex is completely formed. By using this equation, a linear dependence of  $1/(\Phi_f^0 - \Phi_{f(ob)}^0)$  on the concentration of C<sub>60</sub> can be obtained. After linear fit, the constant  $K$  is calculated from the slope. The  $K$  value is 58600 M<sup>-1</sup>.

After removing free C<sub>60</sub> in solution by repeated centrifugation and ultrasonication, the successful intercalation of C<sub>60</sub> on **P-C<sub>10</sub>-GNR** was further examined by monitoring their characteristic UV-vis absorption spectra peak (see Figure 8 top), whereas spectroscopic evidence of C<sub>60</sub> could not be found in **P-GNR** when insertion of C<sub>60</sub> was performed under the same experimental conditions. TEM provides direct evidence for the C<sub>60</sub> intercalation. As shown in Figure 8 bottom, a sharp boundary can be observed between the edge of **P-C<sub>10</sub>-NR** and the supporting carbon film (A), while a thin layer can be

1 identified on the nanorod surface (B) after the addition of  $C_{60}$  followed by removing free  $C_{60}$  molecules  
2 in solution, supporting the conjecture of the sandwiched  $C_{60}$  molecules in the hybrid GNRs. The  
3 combination of  $C_{10}H_{21}SH$  molecules and **P-C<sub>10</sub>-GNR** enabled the insertion of  $C_{60}$ , creating the electron  
4 donor-acceptor alternative structure on the GNR surface. A schemetic illustration of this hybrid structure  
5 donor-acceptor alternative structure on the GNR surface. A schemetic illustration of this hybrid structure  
6 has been presented in Figur 9.  
7  
8  
9  
10



21  
22  
23  
24  
25  
26  
27  
28  
29 **Figure 9.** Schemetic representation of **P-C<sub>10</sub>-GNR** intercalated with  $C_{60}$  and chemical structure of our  
30 synthesized porphyrin thiol **1** and commercially available 1-decanethiol.  
31  
32  
33

34 Structural details of thiol molecules on **P-C<sub>10</sub>-GNR** and **P-GNR** were described in Figure 10, which  
35 showed the feasibility of intercalating  $C_{60}$  between porphyrin molecules on **P-C<sub>10</sub>-GNR** but not on **P-**  
36 **GNR**. Due to the curvature of the small spherical GNPs (*ca.* 2 nm), there was a suitable void space for  
37  $C_{60}$  to insert between two porphyrin groups.<sup>18</sup> In the case of **P-GNR**, the surface curvature is insufficient  
38 to provide such a void space. On GNR surface, the average distance between two gold atoms to which  
39 thiol molecules are attached is about 5 Å.<sup>19</sup> For **P-C<sub>10</sub>-GNR**, between two **1** molecules it is about 10 Å  
40 with one  $C_{10}H_{21}SH$  molecule standing in the middle. From center of porphyrin **1** to the surface of GNR,  
41 it is about 26 Å and the longest chain length of  $C_{10}H_{21}SH$  is 13.4 Å away from the GNR surface. It can  
42 be calculated as 12.6 Å from the center of porphyrin ring to  $C_{10}H_{21}SH$  chain, which is much larger than  
43 7.1 Å, the diameter of a  $C_{60}$  molecule.<sup>18</sup> The closest distance between a carbon of  $C_{60}$  and the center of  
44 the porphyrin ring has been reported as 2.856 Å.<sup>20</sup> The smallest center-to-center distance of two  
45  
46  
47  
48  
49  
50  
51  
52  
53  
54  
55  
56  
57  
58  
59  
60



porphyrin chromophores which can sandwich a  $C_{60}$  molecule is about 12.8 Å by adding the diameter of  $C_{60}$  to twice the closest distance between  $C_{60}$  and a porphyrin ring. With the flexible n-alkyl part of **1** which has 11  $CH_2$  units, the two **1** molecules on **P-C<sub>10</sub>-GNR** can tilt slightly to accommodate a  $C_{60}$  molecule, as shown in the top left picture. On the other hand, for **P-GNR**, since there is no short chain on the surface to provide the void space,  $C_{60}$  molecules could not be sandwiched by porphyrin molecules. The section view of GNR has also been presented to illustrate the feasible intercalation of  $C_{60}$  on **P-C<sub>10</sub>-GNR** and infeasible intercalation on **P-GNR**. The lengths of porphyrin molecule **1** and  $C_{10}H_{21}SH$  were calculated in Chem 3D of ChemDraw.

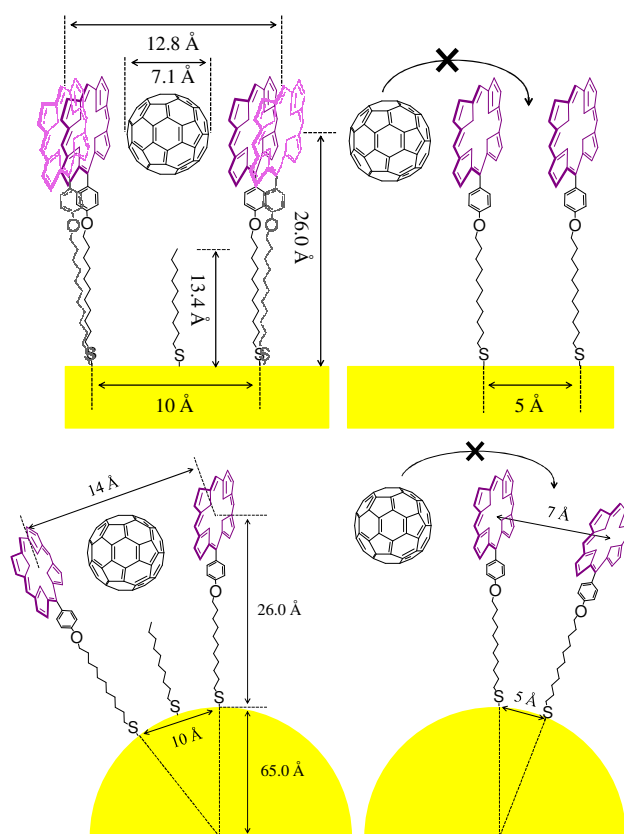


**Figure 10.** Schematic interpretation of feasible intercalation of  $C_{60}$  into **P-C<sub>10</sub>-GNR** instead of **P-GNR**.

The top pictures are from the side view of GNR, and the bottom pictures are from the section view. The *t*-butylphenyl groups at porphyrin core are omitted for clarity.

## CONCLUSION

In conclusion, porphyrin mixed monolayer-protected GNRs were for the first time synthesized and characterized. The resulting porphyrin GNRs showed unique optical properties in sharp contrast to their

1 corresponding spherical GNPs. With the short alkyl thiol molecules, **P-C<sub>10</sub>-GNR** enabled the insertion  
2 of C<sub>60</sub>, creating the electron donor-acceptor alternative structure on the GNR surface. Through this  
3 hybrid nanomaterial, it opens a new avenue for research in investigating the effects of functional organic  
4 molecules on the plasmonic properties of anisotropic gold nanoparticles. This hybrid structure holds  
5 promise for energy conversion in hybrid photovoltaic devices by providing increasing donor-acceptor  
6 interface for the porphyrin-C<sub>60</sub> system with the huge contact area. In addition, for the future study, when  
7 shorten the alkyl of porphyrin thiols and *n*-alkyl chains which pull the porphyrin groups and C<sub>60</sub>  
8 molecules closer to GNR surface (<1 nm), the nanorod structure could be used as a direct path for  
9 charge transport, a key requirement for efficient photovoltaic devices. This combination of organic  
10 electron donor-acceptor system and inorganic NRs could be used to enhance the capability of  
11 photovoltaic devices and improve their performances.  
12  
13  
14  
15  
16  
17  
18  
19  
20  
21  
22  
23  
24

## 25 26 27 ACKNOWLEDGMENT

28  
29  
30  
31 This work was supported by the Air Force Office of Scientific Research (AFOSR FA9550-09-1-  
32 0254). Discussions with X. Ma and Y. Li were acknowledged. The TEM data were obtained at the  
33 (cryo) TEM facility at the Liquid Crystal Institute, Kent State University, supported by the Ohio  
34 Research Scholars Program Research Cluster on Surfaces in Advanced Materials.  
35  
36  
37  
38  
39

40  
41 **Supporting Information Available:** Details of thiol synthesis, the interpretation of successful  
42 synthesis of **1**, Raman spectra, EDX spectra and TEM images of **P-C<sub>10</sub>-GNR** with larger size scale bars.  
43 This material is available free of charge via the Internet at <http://pubs.acs.org>.  
44  
45  
46  
47  
48

## 49 REFERENCES

50  
51  
52 (1) (a) Murphy, C. J.; San, T. K.; Gole, A. M.; Orendorff, C. J.; Gao, J. X.; Gou, L.; Hunyadi, S. E.;  
53 Li, T. Anisotropic Metal Nanoparticles: Synthesis, Assembly, and Optical Applications. *J. Phys. Chem.*  
54 *B* **2005**, *109*, 13857-13870. (b) Burda, C.; Chen, X. B.; Narayanan, R.; El-Sayed, M. A. Chemistry and  
55 Properties of Nanocrystals of Different Shapes. *Chem. Rev.* **2005**, *105*, 1025-1102. (c) Zhou, J.; Dong,  
56  
57  
58  
59  
60

1 J.; Wang, B.; Koschny, T.; Kafesaki, M.; Soukoulis, C. M. Negative Refractive Index due to Chirality.

2  
3 *Phys. Rev. B* **2009**, *79*, 121104.

4  
5 (2) (a) Li, C. Z.; Male, K. B.; Hrapovic, S.; Luong, J. H. T. Fluorescence Properties of Gold  
6 Nanorods and Their Application for DNA Biosensing. *Chem. Commun.* **2005**, 3924-3926. (b) Yu, C. X.;  
7 Irudayaraj, J. Multiplex Biosensor Using Gold Nanorods. *Anal. Chem.* **2007**, *79*, 572-579. (c) Sudeep, P.  
8 K.; Joseph, S. T. S.; Thomas, K. G. Selective Detection of Cysteine and Glutathione Using Gold  
9 Nanorods. *J. Am. Chem. Soc.* **2005**, *127*, 6516-6517.

10  
11 (3) (a) Huang, X. H.; El-Sayed, I. H.; Qian, W.; El-Sayed, M. A. Cancer Cell Imaging and  
12 Photothermal Therapy in The Near-Infrared Region by Using Gold Nanorods. *J. Am. Chem. Soc.* **2006**,  
13 *128*, 2115-2120. (b) Pissuwan, D.; Valenzuela, S. M.; Miller, C. M.; Cortie, M. B. A Golden Bullet?  
14 Selective Targeting of Toxoplasma Gondii Tachyzoites Using Anti Body-Functionalized Gold  
15 Nanorods. *Nano Lett.* **2007**, *7*, 3808-3812. (c) Ding, H.; Yong, K. T.; Roy, I.; Pudavar, H. E.; Law, W.  
16 C.; Bergey, E. J.; Prasad, P. N. Gold Nanorods Coated with Multilayer Polyelectrolyte as Contrast  
17 Agents for Multimodal Imaging. *J. Phys. Chem. C* **2007**, *111*, 12552-12557.

18  
19 (4) (a) Chen, C. C.; Lin, Y. P.; Wang, C. W.; Tzeng, H. C.; Wu, C. H.; Chen, Y. C.; Chen, C. P.;  
20 Chen, L. C.; Wu, Y. C. DNA-Gold Nanorod Conjugates for Remote Control of Localized Gene  
21 Expression by Near Infrared Irradiation. *J. Am. Chem. Soc.* **2006**, *128*, 3709-3715. (b) Tong, L.; Zhao,  
22 Y.; Huff, T. B.; Hansen, M. N.; Wei, A.; Cheng, J. X. Gold Nanorods Mediate Tumor Cell Death by  
23 Compromising Membrane Integrity. *Adv. Mater.* **2007**, *19*, 3136-3141. (c) Norman, R. S.; Stone, J. W.;  
24 Gole, A.; Murphy, C. J.; Sabo-Attwood, T. L. Targeted Photothermal Lysis of The Pathogenic Bacteria,  
25 Pseudomonas Aeruginosa, with Gold Nanorods. *Nano Lett.* **2008**, *8*, 302-306.

26  
27 (5) Daniel, M. C.; Astruc, D. Gold Nanoparticles: Assembly, Supramolecular Chemistry, Quantum-  
28 Size-Related Properties, and Applications toward Biology, Catalysis, and Nanotechnology. *Chem. Rev.*  
29 **2004**, *104*, 293-346.

1  
2  
3  
4  
5  
6  
7  
8  
9  
10  
11  
12  
13  
14  
15  
16  
17  
18  
19  
20  
21  
22  
23  
24  
25  
26  
27  
28  
29  
30  
31  
32  
33  
34  
35  
36  
37  
38  
39  
40  
41  
42  
43  
44  
45  
46  
47  
48  
49  
50  
51  
52  
53  
54  
55  
56  
57  
58  
59  
60

(6) Link, S.; El-Sayed, M. A. Spectral Properties and Relaxation Dynamics of Surface Plasmon Electronic Oscillations in Gold and Silver Nanodots and Nanorods. *J. Phys. Chem. B* **1999**, *103*, 8410-8426.

(7) Yu, C.; Irudayaraj, J. Quantitative Evaluation of Sensitivity and Selectivity of Multiplex NanoSPR Biosensor Assays. *Biophys. J.* **2007**, *93*, 3684-3692.

(8) Nikoobakht, B.; Wang, J. P.; El-Sayed, M. A. Surface-Enhanced Raman Scattering of Molecules Adsorbed on Gold Nanorods: Off-Surface Plasmon Resonance Condition. *Chem. Phys. Lett.* **2002**, *366*, 17-23.

(9) Ni, W. H.; Yang, Z.; Chen, H. J.; Li, L.; Wang, J. F. Coupling Between Molecular and Plasmonic Resonances in Freestanding Dye-Gold Nanorod Hybrid Nanostructures. *J. Am. Chem. Soc.* **2008**, *130*, 6692-6693.

(10) (a) Khanal, B. P.; Zubarev, E. R. Rings of Nanorods. *Angew. Chem. Int. Ed.* **2007**, *46*, 2195-2198. (b) Dai, Q.; Coutts, J.; Zou, J. H.; Huo, Q. Surface Modification of Gold Nanorods through A Place Exchange Reaction inside An Ionic Exchange Resin. *Chem. Commun.* **2008**, 2858-2860. (c) Li, Y. N.; Yu, D. S.; Dai, L. M.; Urbas, A.; Li, Q. Organo-Soluble Chiral Thiol-Monolayer-Protected Gold Nanorods. *Langmuir* **2011**, *27*, 98-103. (d) El Khoury, J. M.; Zhou, X.; Qu, L. T.; Dai, L. M.; Urbas, A.; Li, Q. Organo-Soluble Photoresponsive Azo Thiol Monolayer-Protected Gold Nanorods. *Chem. Commun.* **2009**, 2109-2111. (e) Donkers, R. L.; Lee, D.; Murray, R. W. Synthesis and Isolation of The Molecule-Like Cluster Au<sub>38</sub>(PhCH<sub>2</sub>CH<sub>2</sub>S)<sub>24</sub>. *Langmuir* **2004**, *20*, 1945-1952.

(11) Kadish, K. M.; Smith, K. M.; Guillard, R. *Eds. The Porphyrin Handbook*, Academic Press: San Diego, **2000**.

(12) Sun, Q.; Dai, L.; Zhou, X.; Li, L.; Li, Q. Bilayer- and Bulk-Heterojunction Solar Cells Using Liquid Crystalline Porphyrins as Donors by Solution Processing. *Appl. Phys. Lett.* **2007**, *91*, 253505.

1 (13) (a) Imahori, H.; Arimura, M.; Hanada, T.; Nishimura, Y.; Yamazaki, I.; Sakata, Y.; Fukuzumi, S.  
2 Photoactive Three-Dimensional Monolayers: Porphyrin-Alkanethiolate-Stabilized Gold Clusters. *J. Am.*  
3 *Chem. Soc.* **2001**, *123*, 335-336. (b) Imahori, H.; Kashiwagi, Y.; Endo, Y.; Hanada, T.; Nishimura, Y.;  
4 Yamazaki, I.; Araki, Y.; Ito, O.; Fukuzumi, S. Structure and Photophysical Properties of Porphyrin-  
5 Modified Metal Nanoclusters with Different Chain Lengths. *Langmuir* **2004**, *20*, 73-81.  
6  
7  
8  
9  
10  
11

12 (14) (a) Zhou, X.; Kang, S. W.; Kumar, S.; Kulkarni, R. R.; Cheng, S. Z. D.; Li, Q. Self-Assembly of  
13 Porphyrin and Fullerene Supramolecular Complex into Highly Ordered Nanostructure by Simple  
14 Thermal Annealing. *Chem. Mater.* **2008**, *20*, 3551-3553. (b) Sun, D.; Tham, F. S.; Reed, C. A.; Chaker,  
15 L.; Boyd, P. D. W. Supramolecular Fullerene-Porphyrin Chemistry. Fullerene Complexation by  
16 Metalated "Jaws Porphyrin" Hosts. *J. Am. Chem. Soc.*, **2002**, *124*, 6604-6612 and references there in.  
17  
18  
19  
20  
21  
22  
23  
24

25 (15) (a) Brust, M.; Walker, M.; Bethell, D.; Schiffrin, D. J.; Whyman, R. Synthesis of Thiol-  
26 Derivatized Gold Nanoparticles in A 2-Phase Liquid-Liquid System. *J. Chem. Soc. Chem. Commun.*  
27 **1994**, 801-802. (b) Zhou, X.; El Khoury, J. M.; Qu, L.; Dai, L.; Li, Q. A Facile Synthesis of Aliphatic  
28 Thiol Surfactant with Tunable Length as A Stabilizer of Gold Nanoparticles in Organic Solvents. *J.*  
29 *Colloid Interf. Sci.* **2007**, *308*, 381-384.  
30  
31  
32  
33  
34  
35  
36  
37

38 (16) Huang, X. H.; Neretina, S.; El-Sayed, M. A. Gold Nanorods: From Synthesis and Properties to  
39 Biological and Biomedical Applications. *Adv. Mater.* **2009**, *21*, 4880-4910.  
40  
41  
42

43 (17) Park, H. S.; Agarwal, A.; Kotov, N. A.; Lavrentovich, O. D. Controllable Side-by-Side and End-  
44 to-End Assembly of Au Nanorods by Lyotropic Chromonic Materials. *Langmuir* **2008**, *24*, 13833-  
45 13837.  
46  
47  
48  
49

50 (18) Hasobe, T.; Imahori, H.; Kamat, P. V.; Ahn, T. K.; Kim, S. K.; Kim, D.; Fujimoto, A.;  
51 Hirakawa, T.; Fukuzumi, S. Photovoltaic Cells Using Composite Nanoclusters of Porphyrins and  
52 Fullerenes with Gold Nanoparticles. *J. Am. Chem. Soc.* **2005**, *127*, 1216-1228.  
53  
54  
55  
56  
57  
58  
59  
60

1 (19) (a) Poirier, G. E. Characterization of Organosulfur Molecular Monolayers on Au(111) Using  
2 Scanning Tunneling Microscopy. *Chem. Rev.* **1997**, *97*, 1117-1127. (b) Menendez, G.; Cortes, E.;  
3 Grumelli, D.; De Leo, L. P. M.; Williams, F. J.; Tognalli, N. G.; Fainstein, A.; Vela, M. E.; Jares-  
4 Erijman, E. A.; Salvarezza, R. C. Self-Assembly of Thiolated Cyanine Aggregates on Au(111) and Au  
5 Nanoparticle Surfaces. *Nanoscale* **2012**, *4*, 531-540.  
6  
7  
8  
9  
10

11  
12 (20) Sun, D. Y.; Tham, F. S.; Reed, C. A.; Chaker, L.; Burgess, M.; Boyd, P. D. W. Porphyrin-  
13 Fullerene Host-Guest Chemistry. *J. Am. Chem. Soc.* **2000**, *122*, 10704-10705.  
14  
15  
16  
17  
18  
19  
20  
21  
22  
23  
24

25 TOC:

